EPR study of hydrogen ions in stressed CaO crystals

S. C. Ke and H. T. Tohver
Physics Department, University of Alabama at Birmingham, Birmingham, Alabama 35294
(Received 17 November 1994; revised manuscript received 25 April 1995)

The H^{2-} ion in CaO is paramagnetic and has an isotropic electron paramagnetic resonance spectrum above 13 K. Below 13 K, the defect symmetry is tetragonal with ⟨001⟩ as the symmetry axis. In this present work, the EPR spectrum of H^{2-} in a stressed sample at 13 K has the same symmetry and spin-Hamiltonian parameters as of unstressed samples at 4 K. The strain results in a preferential alignment of the centers along the stretch axis—the ⟨001⟩. The superhyperfine interaction with the magnetic ^{43}Ca isotopes in the [001] plane yields $|A_\perp|=11.0\pm0.1$ MHz, $|A_\parallel|=9.1\pm0.1$ MHz with the symmetry axis along the ⟨100⟩ or ⟨010⟩. A model consistent with the results is a T_{1u} ground state with the degeneracy lifted by a static tetragonal Jahn-Teller distortion of the lattice that becomes apparent below 13 K.

I. INTRODUCTION

Study of substitutional hydrogen ions in MgO and CaO crystals has evoked considerable interest during the past ten years.[1–9] These centers consist of a proton surrounded by either two or three electrons and occupy an oxygen vacancy. With two electrons in the vacancy, a region of local positive charge exists, which can act as an electron trap. It has been shown that these H^- defects are the main traps for electrons excited from F centers and are responsible for a long-lived luminescence. This reversible process was described as[10]

$$F+h\nu\leftrightarrow F^*\leftrightarrow F^+ + e^- , \tag{1}$$

$$e^- + H^- \leftrightarrow H^{2-} . \tag{2}$$

The optically generated F^+ centers and the H^{2-} ions then each have one unpaired electron and, hence, are amenable to electron paramagnetic resonance (EPR) techniques. The presence of the H^{2-} ion was verified by the EPR spectroscopy of deuterium-enriched MgO (Ref. 11) and CaO (Ref. 12) crystals. In CaO, above 13 K, the EPR spectrum associated with the H^{2-} ion consists of two iosotropic lines centered at $g\cong 2$. Extended study[13] of this EPR signal at liquid-helium temperature reveals tetragonal symmetry along the ⟨001⟩ crystal axis. A $[H^-Ca^+]$ model to account for the symmetry lowering was proposed by Orera, Sanjuan, and Chen,[13] in which the unpaired electron is localized in the 4s orbital of one of the calcia sites surrounding the substitutional H^- ion.

However, based on electronic-structure calculations, an alternative model was proposed by Rõõm[14] and Hsu,[15] in which the unpaired electron is located at the vacancy site with the T_{1u} ground state. The Jahn-Teller or pseudo-Jahn-Teller effect, including the 2s-2p hybridization in the H^{2-} ion, would then further lower the symmetry.

To resolve the conflicts between these two models, (1) we show the effect of stress on the H^{2-} ion at 13 K and discuss the problem concerning the structure of H^{2-} centers in CaO, and (2) we report the observation and analysis of the satellite structure associated with the H^{2-} EPR signals.

II. EXPERIMENTAL DATA

The CaO crystals were grown at the Oak Ridge National Laboratory using the arc-fusion method. Defects resulting from additive coloration of CaO crystals at high temperature and at high pressure of calcium vapors are primarily F centers and substitutional H^- ions.[16,17]

The sample was cleaved along the principal axis with dimensions of $7\times7\times0.5$ mm^3 The [001] crystal plane was epoxied to an oxygen-free high-conductivity copper rod. The stress on the sample was generated by the contraction at low temperature,[18] which is larger for copper than for CaO. Hence the sample was equally compressed along the ⟨100⟩ and ⟨010⟩ crystal directions. This process is equivalent to stretching along the ⟨001⟩ axis and yields a tetragonal distortion.

At 45 K, the stress-generated shifts δH of the $(m_s=\pm\frac{1}{2}\rightarrow m_s=\pm\frac{3}{2})$ fine structure lines of Mn^{2+} EPR spectra are 6.5 G. Using Feher's[19] results of the stress shifts of Mn^{2+} lines in MgO, we can make a rough estimate of the thermal stress in our samples at 45 K. According to her analysis, for $B\|\langle001\rangle$ and stress along ⟨001⟩,

$$\delta H=\tfrac{3}{2}\times C_{11}\times P , \tag{3}$$

where C_{11} is a spin-lattice coupling constant and P is the stress. We estimate[20,21] C_{11} to be 9.2×10^{-13} cm/dyn for the Mn^{2+} ion in CaO—comparable with Feher's result[19] of 7.3×10^{-13} cm/dyn for Mn^{2+} in MgO. We therefore estimate our stress at 45 K and below to be of the order of 5×10^2 kg/cm^2.

To enhance the H^{2-} concentration, the sample was illuminated with 420-nm light. The light source was a 500-W high-pressure mercury arc lamp fitted with an Oriel 7210 grating monochromator.

The EPR spectra were taken with a Bruker Associates SRC 200 spectrometer operating at 9.76 GHz. Sample temperatures were controlled by an Air Products model DMX-1A/15 closed-cycle helium refrigerator.

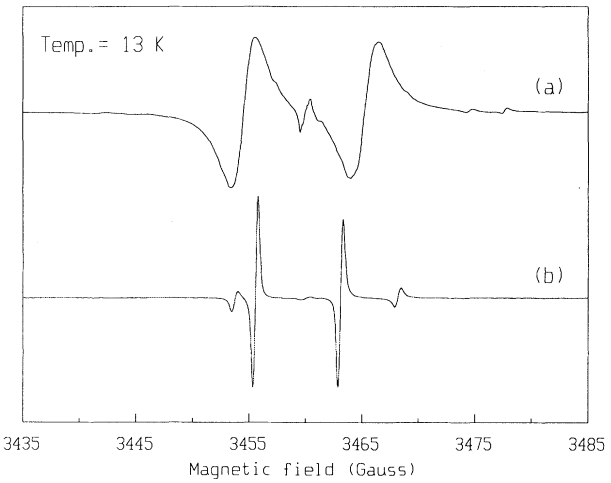

FIG. 1. (a) H^{2-} EPR signals from an unstressed sample at 13 K showing the motional averaging effect. The line at the center corresponds to the saturated F^+ signal. (b) Stretching manifests itself not only in the symmetry lowering but also in the induced preferential alignment of centers along the stretch axis. The two inner lines correspond to the defect axis perpendicular to the magnetic field, while the outer two correspond to the parallel direction. The spectrum is measured with $B\|\langle 100\rangle$ and $P\|\langle 001\rangle$.

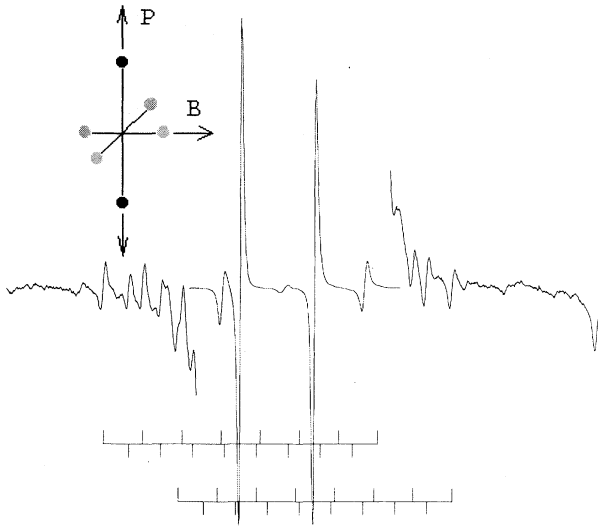

FIG. 2. Hyperfine group (central part) of the H^{2-} measured with $B\|\langle 100\rangle$ and $P\|\langle 001\rangle$ at 13 K showing the ^{43}Ca superhyperfine lines (outer part). The SHFS in the central region is submerged in the H^{2-} hyperfine signals. The electronic receiver gain of the outer part is 250 times higher than the central part. Diagram on the upper left shows the crystal orientation of the measured EPR spectrum. The stick diagram at the bottom refers to the SHFS positions of lines corresponding to the two highly populated H^{2-} lines.

III. RESULTS

A. Strain effect

At 13 K, stretching along the $\langle 001\rangle$ axis produces a strain in the crystal and lowers the symmetry from cubic to tetragonal. The resultant H^{2-} EPR spectrum (Fig. 1) at 13 K has the same symmetry and spin-Hamiltonian parameters as the unstressed sample at 4 K by Orera, Sanjuan, and Chen.[13] EPR constants from various sources are listed in Table I. Analysis of the liquid-helium temperature spectrum, including the fact that the lines from forbidden nuclear transitions due to the hydrogen nuclear Zeeman term and the H^{2-} hyperfine interaction are of similar strength, has been thoroughly done by Orera, Sanjuan, and Chen.[13]

In addition, the effect of the strain causes the strength of the H^{2-} EPR lines corresponding to centers along the stretch axis to grow at the expense of the other two. The intensity of a paramagnetic resonance line is a direct measure of the number of H^{2-} centers of corresponding orientation. We designate the number of centers parallel to the stretch axis by $N(\theta=0°)$, the number of centers perpendicular to the stretch axis by $N(\theta=90°)$, and the energy difference between these two orientations as ΔU. Through the Boltzmann statistics,

$$\Delta U = kT \times \ln\left[\frac{N(\theta=0°)}{\frac{1}{2}N(\theta=90°)}\right], \qquad k = \text{Boltzmann's constant} \quad (4)$$

we find $\Delta U = 2.5\pm0.4$ meV. This ΔU is greater than kT at 13 K.

B. Superhyperfine structure

Figure 2 displays the satellites of the two highly populated H^{2-} EPR lines, with the external magnetic field $B\|\langle 100\rangle$ and the stretch axis $P\|\langle 001\rangle$ crystal direction. The two intense H^{2-} lines are each flanked by two sets of eight equally spaced lines of equal intensity. We attribute these satellites to the hyperfine interaction of the electron spin in the H^{2-} defect with those magnetic ^{43}Ca isotopes ($I=\frac{7}{2}$) in the [001] plane. We have not observed any hyperfine interaction with the two Ca ions along the stretch axis $\langle 001\rangle$.

TABLE I. Spin-Hamiltonian parameters of H^{2-} centers in the CaO crystal.

Temperature	$g_\|$	$g_\perp$	g	$A_\|$ (MHz)	$A_\perp$ (MHz)	A (MHz)	Ref.
30 K			2.0002			28.5	12
4 K unstressed	1.9996	2.0005		40.3±1.6	20.9±0.8		13
4 K unstressed	1.9996(2)	2.0003(2)		41.2±0.2	21.4±0.2		15
13 K stressed	1.9995(1)	2.0005(1)		40.3±0.6	21.4±0.4		This work

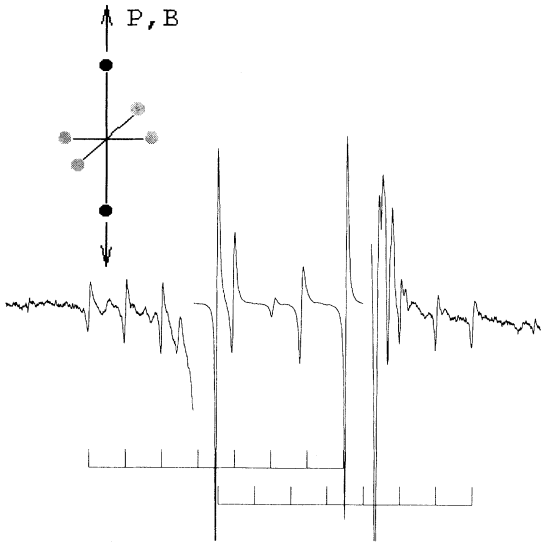

FIG. 3. Hyperfine group (central part) of the H^{2-} measured with $B\|\langle 001\rangle$ and $P\|\langle 001\rangle$ at 13 K showing the ^{43}Ca superhyperfine lines (outer part).

Two different planes of rotation of B were employed to study the superhyperfine structure (SHFS) orientation dependence with respect to the stretch (P) and magnetic field (B) axes. The stretch axis P is taken as the $\langle 001\rangle$ crystal direction.

(1) B rotates in the [010] plane—containing the stretch axis: As the magnetic field B departs from the $\langle 100\rangle$ direction, one set of eight lines remain fixed, while the other set moves towards and collapses with the fixed set when the magnetic field B becomes parallel to the stretch axis P (Fig. 3).

(2) B rotates in the [001] plane—normal to the stretch axis: Two sets of SHFS are observed when the magnetic field is parallel to the $\langle 100\rangle$ axis; they move toward each other as the magnetic field departs from the $\langle 100\rangle$ direction. With $B\|\langle 110\rangle$, these two sets of lines coincide (Fig. 4).

These two orientation dependence studies both reveal axial symmetry about the $\langle 100\rangle$ or $\langle 010\rangle$ crystal axes for the A tensor, as shown in Figs. 5(a) and 5(b).

The EPR spectra are fitted to the following superhyperfine spin Hamiltonian:

$$\mathcal{H}^{43}Ca = A_{\|}S_zI_z + A_{\perp}(S_xI_x + S_yI_y)\,, \tag{5}$$

with $S=\frac{1}{2}$, $I=\frac{7}{2}$, $|A_{\perp}|=11.2\pm0.1$ MHz, and $|A_{\|}|=9.1\pm0.1$ MHz. The absolute sign of the hyperfine constants cannot be obtained from the spectra.

The natural abundance of the ^{43}Ca ($I=\frac{7}{2}$) isotope is

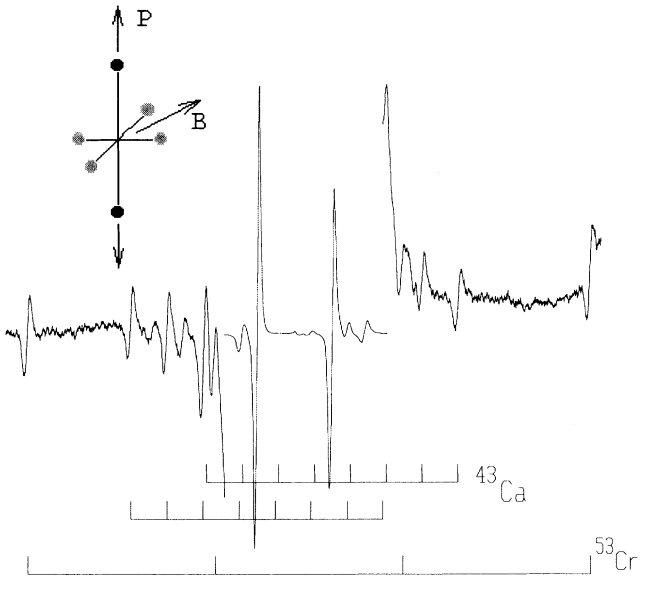

FIG. 4. Hyperfine group (central part) of the H^{2-} measured with $B\|\langle 110\rangle$ and $P\|\langle 001\rangle$ at 13 K showing the ^{43}Ca superhyperfine lines (outer part). The hyperfine structure due to ^{53}Cr is indicated.

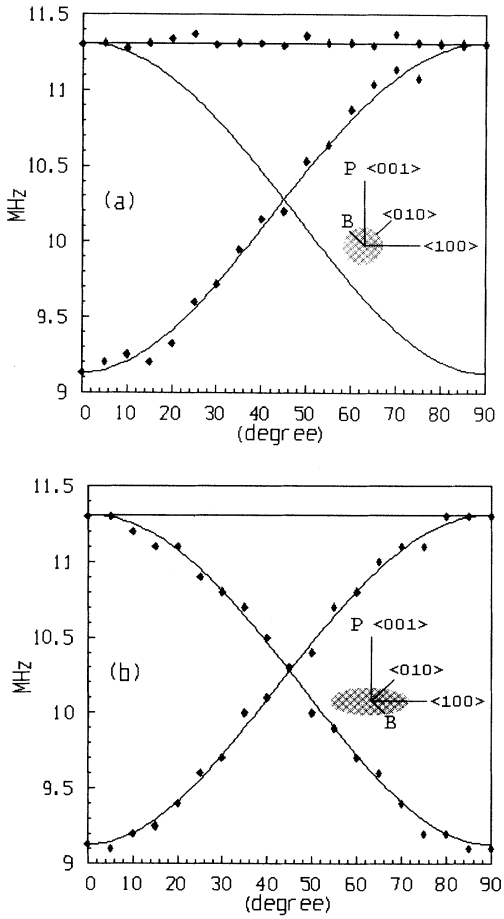

FIG. 5. (a) tensor angular dependence for B rotating in the [010] plane and $P\|\langle 001\rangle$. ♦ are the experimentally detected values and the lines are the calculated ones. (b) tensor angular dependence for B rotating in the [001] plane and $P\|\langle 001\rangle$. ♦ are the experimentally detected values and the lines are the calculated ones.

TABLE II. First-neighbor hyperfine-interaction parameters.

Defect	Nucleus	a (MHz)	b (MHz)	$\langle R \rangle$ Å	$10^{-20}\lvert\varphi(0)\rvert^2$ (cm^{-3})	Ref.
F^+ in MgO	^{25}Mg	11	1.3		2780	23,24
F^+ in CaO	^{43}Ca	25.66	2.71		5800	25
H^{2-} in MgO	1_H	158			2400	11
	^{25}Mg	30.5	1.1	1.7	7540	6
H^{2-} in CaO at 13 K	^{1}H	28.5				12
$[H^-Ca^+]$ at 4 K	^{1}H	28	6.7	2.3	421	13
H^{2-} in stressed CaO	^{1}H	28	6.7	2.3	421	This work
	^{43}Ca	10.4	0.62	2.1	2330	This work

0.135%. The probability of having one ^{43}Ca isotope among the six Ca ions surrounding the H^{2-} ion is 0.0080, and the probability of having no Ca isotope is 0.9919; therefore, the ratio of probabilities is 0.0081. Since only the four ^{43}Ca of the [001] plane contribute intensities to the observed SHFS, we arrive at an expected ratio of 0.0054 between the sum of intensity of the eight lines and that of the central line. The average observed ratio is 0.0050, which agrees well within the experimental errors. We conclude that the satellite structures are due to the unpaired electron of the H^{2-} ion interacting with the magnetic ^{43}Ca isotopes in the [001] plane with the stretch axis being the $\langle 001 \rangle$.

IV. DISCUSSION

If we decompose the axial superhyperfine A tensor of the electron-calcium interaction into its isotropic and anisotropic components a and b, defined by

$$a=(A_{\parallel}+2A_{\perp})/3 \quad \text{and} \quad b=(A_{\parallel}-A_{\perp})/3 \ , \tag{6}$$

we obtain the values $a=10.4$ MHz and $b=0.62$ MHz. The isotropic hyperfine constant "a" is related to the unpaired electron wave function at the ^{43}C nucleus through the Fermi contact term

$$a=(8\pi/3h)[g_e\beta_e][g_N\beta_N]|\varphi(0)|^2 \ , \tag{7}$$

where $|\varphi(0)|^2$ is the electron spin density at the ^{43}Ca nucleus. We obtain $|\varphi(0)|^2=2330\times10^{20}$ cm^{-3}, which is approximately five times higher than the value at the proton site.

The observed isotropic hyperfine constant a of 10.4 MHz is about 60 times smaller than in the 4s orbital of atomic calcia (640.7 MHz).[22] Thus, the unpaired electron cannot be localized in the 4s orbital of the calcia site.

The point dipole approximation, using $b=(1/h)[g_e\beta_e][g_N\beta_N](1/R^3)$, gives an electron-calcium distance $R=2.1$ Å in the [001] plane. Values of spin density at the nucleus and electron-nuclear dipole-dipole distances of F^+ and H^{2-} defects of various works are summarized in Table II. We speculate that the large difference in the H hyperfine interaction for MgO and CaO is mainly due to the difference in the lattice constants. However, attempts to draw more information from the experimental data reported in this paper would tend to be fraught with ambiguities.

In stressed CaO at 13 K, the observation of axial superhyperfine splitting by ^{43}Ca nucleus places the proton and three electrons in the oxygen vacancy. This defect configuration of H^{2-} in CaO is the same as was proposed for MgO.[6] The electronic structure calculations done independently by Hsu[14] and Room[15] have shown that the H^{2-} ground state in the cubic-symmetric unrelaxed CaO host is of the orbitally degenerate T_{1u} type. In a cubic host crystal, the direct product $[T_{iu}]^2$ contains A_{1g}, E_g, and T_{2g}. The A_{1g} mode does not induce splitting of the electronic states. Hence, depending on the relative coupling strength of the E_g and T_{2g} modes, two types of static Jahn-Teller distortions are possible, tetragonal and trigonal deformation of the cluster, respectively.[26,27] The consistency between the EPR results for the externally stressed sample at 13 K and the unstressed sample at 4 K support the interpretation that the E_g mode is the dominant spontaneous Jahn-Teller distortion at 4 K.

Finally, density-functional-based calculations[28] have shown that the state of lowest energy is of D_{4h} symmetry, and, the spin density at the nucleus site is very sensitive to the amount of internuclear relaxation.

V. CONCLUSION

A model for the H^{2-} centers in CaO consistent with the EPR results and electronic structure calculations is that the configuration of the hydrogen defect in CaO is a proton with three electrons centered in the oxygen vacancy. At 13 K and above the center is isotropic because of motional averaging known before.[12,13] Below 13 K (or at 4 K) the T_{1u} ground state has the threefold degeneracy removed by a tetragonal (E_g) Jahn-Teller distortion of the lattice.

ACKNOWLEDGMENTS

The CaO crystals were kindly supplied by Dr. Y. Chen of the Oak Ridge National Laboratories. The authors gratefully acknowledge illuminating discussions with Dr. Joseph Harrison about this model.

[1]R. Gonzalez, Y. Chen, and M. Mostoller, Phys. Rev. B **24**, 6862 (1981).
[2]M. M. Abraham, Y. Chen, D. N. Olson, V. M. Orera, T. M. Wilson, and R. F. Wood, Phys. Rev. B **23**, 51 (1981).
[3]G. P. Summers, T. M. Wilson, B. T. Jeffries, H. T. Tohver, Y. Chen, and M. M. Abraham, Phys. Rev. B **27**, 1283 (1983).
[4]R. Gonzalez, G. P. Summers, and Y. Chen, Phys. Rev. B **30**, 2112 (1983).
[5]John F. Boas and John R. Pilbrow, Phys. Rev. B **32**, 8258 (1985).
[6]V. M. Orera and Y. Chen, Phys. Rev. B **36**, 5576 (1987).
[7]V. M. Orera and Y. Chen, Phys. Rev. B **36**, 6120 (1987).
[8]T. Rõõm, and G. Liidja, Radiat. Eff. Defects Solids **119-121**, 855 (1991).
[9]T. Rõõm, and G. Liidja, Proc. Estonian Acad. Sci. Phys. Math. **41**(1), 49 (1992).
[10]V. M. Orera and Y. Chen, Phys. Rev. B **36**, 1244 (1987).
[11]J. Tombrello, H. T. Tohver, Y. Chen, and T. M. Wilson, Phys. Rev. **30**, 7374 (1984).
[12]J. Tombrello, H. T. Tohver, and Y. Chen, Bull. Am. Phys. Soc. **31**, 529 (1986).
[13]V. M. Orera, M. L. Sanjuan, and Y. Chen, Phys. Rev. B **42**, 7604 (1991).
[14]T. Rõõm, Ph. D. thesis, University of Tartunsis, Tallinn, 1993.
[15]J. W. Hsu, Ph. D. thesis, University of Alabama at Birmigham, 1991.
[16]M. M. Abraham, C. T. Butler, and Y. Chen, J. Chem. Phys. **55**, 3752 (1971).
[17]R. Gonzalez, G. P. Summers, and Y. Chen, Phys. Rev. B **30**, 2112 (1984).
[18]At 13 K, the linear contraction of the copper rod is $[\Delta L/L_0 = -0.324\%]$ and of the CaO crystal is $[\Delta L/L_0 = -0.166\%]$. Y. S. Touloukian, R. K. Kirby, R. E. Taylor, and T. Y. R. Lee, *Thermal Expansion-Nonmetallic Solids,* TPRC Data Series, Vol. 13 (IFI/Plenum, New York, 1977).
[19]Elsa Rosenvasser Feher, Phys. Rev. **136**, A145 (1964).
[20]W. G. Penney and R. Schlapp, Phys. Rev. **41**, 194 (1932).
[21]A. E. Hughes and W. A. Runciman, J. Phys. C **2**, 37 (1969).
[22]J. R. Morton and K. F. Preston, J. Magn. Reson. **30**, 577 (1978).
[23]W. P. Unruh and J. W. Culvahouse, Phys. Rev. **154**, 861 (1967).
[24]L. E. Halliburton, D. L. Cowan, and L. V. Holroyd, Phys. Rev. B **12**, 3408 (1975).
[25]B. Henderson and A. C. Tomlinson, J. Phys. Chem. Solids **30**, 1801 (1968).
[26]Shinji Muramatsu and Takeshi Iida, J. Phys. Chem. Solids **31**, 2209 (1970).
[27]M. Bacci, A. Ranfagni, M. P. Fontana, and G. Viliani, Phys. Rev. B **11**, 3052 (1974).
[28]S. C. Ke, D. C. Patton, J. G. Harrison, and H. T. Tohver (to be published).